SELF-CONSISTENT SIMULATION OF QUANTUM TRANSPORT IN DUAL-GATE FIELD-EFFECT TRANSISTORS

J.M. Bigelow, J.P. Leburton and M.H. Degani
Beckman Institute, University of Illinois, Urbana, IL 61801

Abstract

We present the simulation of both the equilibrium conditions and the current characteristics of the dual-gate FET. We use a new numerical technique for computing electronic states in confined micro-systems based on a solution of the time-dependent Schrödinger equation which utilizes propagation of the wave-function in the imaginary time domain. Our results show resonant tunneling peaks and negative differential resistance in the drain-current/gate-source voltage characteristics that are in good agreement with experiment.

The success of resonant tunneling diodes in applications of high-speed circuits has led naturally to the development of three-terminal resonant-tunneling devices. In the dual-gate field-effect transistor (Figure 1a), parallel potential barriers can be induced in a two-dimensional (2D) electron gas of a MODFET structure [1]-[4]. If the gate biases are separate, one barrier can be used as a tunneling injector while the other can be used as an energy spectrometer [1, 4]. With the gates interconnected, Chou et al. have demonstrated negative differential resistance (NDR) in the drain current/gate-source voltage characteristics under illumination at $T = 4.2K$ [2]. Simultaneously, Ismail et al. showed the same characteristics without illumination [3]. The experimental drain-source current versus gate-source bias curve is shown in Figure (2a) where the thermionic emission current has been subtracted [3]. The measurements were taken at $T = 4.2K$ with the drain-source bias set at $0.2\ mV$. The resonant tunneling peaks for the first three quasi-bound states in the wire are clearly seen. In this paper we present a self-consistent Poisson and time-dependent Schrödinger equation solver which successfully simulates both the equilibrium and current characteristics of the dual-gate FET of [3]. The device under consideration is shown schematically in Figure (1a). In this investigation the two gates are connected.

The major difficulty in modeling the current-voltage characteristics of the dual-gate FET resides in an accurate computation of the quasi-bound states between the double-barrier under a lateral electric field. The difficulty is compounded by the presence of a continuum of 2D states outside the barriers. In this analysis, we assume the structure to be periodic in the x-direction and choose the distance of the region outside the barrier to be large enough so that no interaction, either electrostatically or quantum mechanically, occurs between two successive double-barrier wells. Then we consider only the bottom two quasi-bound states and assume a continuum of states outside the barriers starting with the ground state energy level E_{2D}. This approximation greatly simplifies the calculations as seen below.

By imposing periodic boundary conditions in the x-direction, solving the Poisson equation is greatly simplified. With the utilization of Fourier transforms in the x-direction we are able to effectively decouple the x and y-directions in (k_x, y) space, solve the Poisson equation in this space, and then take the inverse Fourier transform in order to obtain the potential in (x, y) space. The success in decoupling the two directions insures quick computations of the

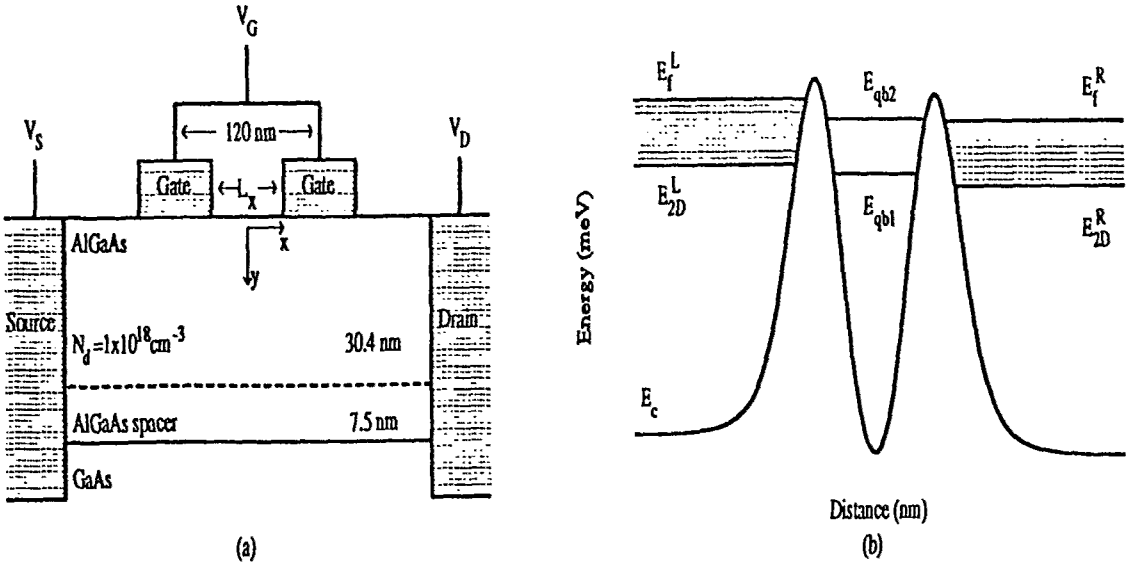

Fig. 1 (a) Schematic diagram of the dual-gate field-effect transistor. (b) The conduction band-edge of a dual-gate FET under source-drain bias showing a net tunnel current due to the imbalance in the energies of electrons between the left and the right side of the double-barrier (shaded regions). The quasi-bound levels are labeled E_{qb1} and E_{qb2}.

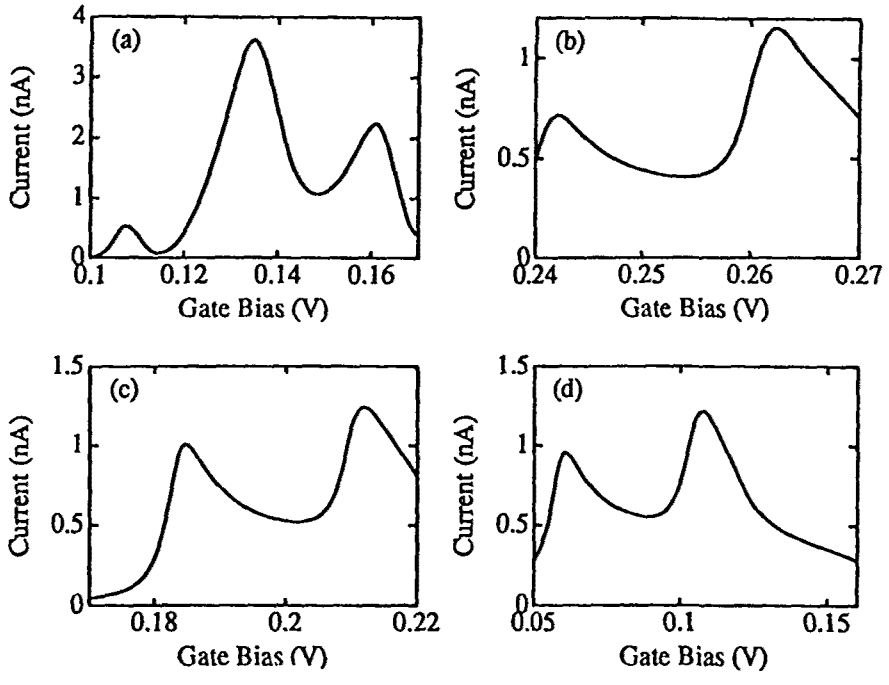

Fig. 2 (a) Experimental resonance drain-source current (After Ismail et. al [3]). Calculated resonance drain-source current as a function of gate bias showing the peaks due to the first two quasi-bound levels for (a) L_x= 600 Å, (b) L_x= 750 Å, and (c) L_x= 900 Å.

Poisson equation.

The method we utilize to obtain the eigenstates of the system in equilibrium is based on the split-operator propagation method [5] using imaginary time propagation [6, 7]. In the split-operator propagation scheme, the kinetic operator and potential operator are used to propagate the wave function separately according to

$$\psi(x,y,t+\Delta t) \simeq e^{-\frac{iV(x,y)\Delta t}{2\hbar}} e^{-\frac{iK_E(x,y)\Delta t}{2\hbar}} e^{-\frac{iV(x,y)\Delta t}{2\hbar}} \psi(x,y,t) \tag{1}$$

for each successive time step Δt. Here $K_E(x,y)$ is the kinetic energy operator and $V(x,y)$ is the electric potential. In this way, the calculation of the wave function for each successive time step is relatively straight forward. The $\exp(-iV(x,y)\Delta t/2\hbar)$ terms are scalar and the K_{Ey} term can be easily calculated by using an approximation given in [6], which reduces to the inversion of a tridiagonal solver with the use of finite difference methods. The kinetic energy operator in the x-direction is more complicated but we can once again take advantage of the periodicity by using Fourier transforms. As with the Poisson equation solver, this method successfully decouples the x and y-directions, allowing quick one-dimensional calculations.

The complete algorithm includes self-consistently solving the Poisson and Schrödinger equations along with the expressions for the charge distribution. The ground state is obtained through the propagation of an initial wave packet according to Equations (1) in imaginary time ($t = -i\tau$), and the excited states are constructed by using Gram-Schmidt orthonormalization, which insures orthonormality between all the states in each time step. Between the barriers, one-dimensional statistics are used to calculate the charge, while outside the barriers, two-dimensional statistics are used. To further simplify the calculations, we assume $T = 0\ K$ because we are at such low temperatures ($T = 4.2\ K$). This means all the occupied states are of the first sublevel family in the y-direction. The scheme is very stable and the convergence is quite fast because the two dimensions have been decoupled.

For the device under the application of a drain-source bias, we assume a linear electric field with no changes in the charge distribution because of the extremely small drain-source voltage ($V_{DS} = 0.2mV$). Under a linear field $F\hat{x}$, the new Hamiltonian reads

$$H = \frac{1}{2m^*}(\frac{\hbar}{i}\nabla - qF\hat{x}\Delta t)^2 + V(x,y). \tag{2}$$

Because the spatial periodicity is maintained, Fourier transform methods can still be utilized. However under the application of an electric field, we now propagate the wave function according to Equation (1) in real-time rather than imaginary time. In this new guage, the quantum mechanical current density carried by the n^{th} quasi-bound state reads

$$j_n = \frac{\hbar}{m^*} Re\left(-i\psi_n^*\nabla\psi_n - \frac{qF\Delta t}{\hbar}\psi_n^*\psi_n\right). \tag{3}$$

The total current from left to right is calculated by integrating j_n over the y and z-directions and summing over all the states above the quasi-Fermi level E_f^L and is given by

$$I_{LR} = 2qL_z\sqrt{\frac{2m^*}{\hbar^2}} \sum_{E_n<E_f^L} \int_y dy\ \ j_n(y)\sqrt{E_f^L - E_{qbn}}. \tag{4}$$

A similar expression for the tunneling current from right to left can be obtained by substituting L for R and R for L in Equation (4). The total current is simply the difference between the two contributions. Figure (1b) shows that if the n^{th} quasi-bound state (E_{qbn}) lies between the Fermi level on the left (E_f^L) and the lowest 2D sublevel (E_{2D}), electrons to the left of the double-barrier can tunnel through that state into the right side of the barrier. From Figure (1b), an increase in gate bias lowers the double-barrier and thus the sublevel E_{qbn}. Because of the difference of the density of states on both sides of the barrier, the tunneling current increases as the sublevel passes below E_f^L until it peaks when it reaches E_f^R. For larger gate-biases, the current decreases until the quasi-bound level passes below E_{2D}, when the current goes to zero.

The device of Figure (1a) was simulated for L_x = 600, 750 and 900 Å . The lowest ten wave-functions of the periodic structure were calculated, which included the two quasi-bound states. Imaginary-time propagation was used in the equilibrium case with a time step of 2.0 fsec. Under the application of V_{DS}, the equilibrium wave-functions are used as the initial wave-functions which are then propagated in real-time with a time step of 0.5 fsec.

The calculated resonance currents are plotted in Figures (2b-2d) for L_x=600 Å, L_x=750 Åand L_x=900 Å, respectively. For gate-biases greater than the ranges shown in Figures (2b-2d), the double-barrier dipped below the quasi-Fermi level which invalidates our approximations for the charge distributions and the tunneling currents. The gate biases corresponding to the peak values of the current suggests that simulation would best match experiment for a L_x value between 750 and 900 Å. This corresponds nicely to the actual device photograph, which shows L_x to be approximately 850 Å[3]. In addition, the current peaks are separated by $0.028V$ for the 750 Å curve, which compares favorably to the experimental separation of $0.027V$ in Figure (2c).

In conclusion, we have modeled the quantum-mechanical current in the double-barrier field-effect transistor with a self-consistent Poisson and Schrödinger equation solver. The simulation shows the characteristic resonance peaks in the drain-source current versus gate-source voltage curves due to tunneling through the quasi-bound states of the double-barrier. The calculated results compare favorably with the experimental results, especially with the current peak separation and the resonance current through the first quasi-bound state.

[1] A. Palevski, M. Heiblum, C.P. Umbach, C.M. Knoedler, A.N. Broers, and R.H. Koch, *Phy. Rev. Lett.*, **62**, 1776-1779, (1989).
[2] S.Y. Chou, D.R. Allee, R.F.W. Pease, and J.S. Harris, Jr., *Appl. Phys. Lett.*, **55**, 176-178, (1989).
[3] K. Ismail, D.A Antoniados, and H.I. Smith, **55**, 589-591, (1989).
[4] U. Sivan, A. Palevski, M. Heiblum, and C.P. Umbach, *Solid-State Elec.*, **33**, 979-986, (1990).
[5] C. Leforestier, R.H. Bisseling, C. Cerjan, M.D. Feit, R. Friesner, A. Guldberg, A. Hammerich, G. Jolicard, W. Karrlein, H.-D. Meyer, N. Lipkin, O. Roncero, and R. Kosloff, *Journ. of Comp. Physics,* **94**, 59-80, (1991).
[6] M. H. Degani, *Appl. Phys. Lett.* **59**, 57-59, (1991).
[7] M. H. Degani and J.P. Leburton *Phys. Rev.* **44**, 10901-10904, (1991).